



HAL
open science

Pathways of anthropogenic carbon subduction in the global ocean

Laurent Bopp, Marina Lévy, Laure Resplandy, Jean-Baptiste Sallée

► **To cite this version:**

Laurent Bopp, Marina Lévy, Laure Resplandy, Jean-Baptiste Sallée. Pathways of anthropogenic carbon subduction in the global ocean. *Geophysical Research Letters*, 2015, 42 (15), pp.6416-6423. 10.1002/2015GL065073 . hal-01211485

HAL Id: hal-01211485

<https://hal.science/hal-01211485>

Submitted on 17 Sep 2020

HAL is a multi-disciplinary open access archive for the deposit and dissemination of scientific research documents, whether they are published or not. The documents may come from teaching and research institutions in France or abroad, or from public or private research centers.

L'archive ouverte pluridisciplinaire **HAL**, est destinée au dépôt et à la diffusion de documents scientifiques de niveau recherche, publiés ou non, émanant des établissements d'enseignement et de recherche français ou étrangers, des laboratoires publics ou privés.



RESEARCH LETTER

10.1002/2015GL065073

Key Points:

- Ninety percent of carbon absorbed over the last decade has been subducted at the base of the mixed layer
- Vertical diffusion is the primary mechanism of subduction, contributing 65% of total subduction
- We suggest a strong need for a better estimate of vertical diffusion intensity in the upper ocean

Correspondence to:

L. Bopp,
Laurent.Bopp@lsce.ipsl.fr

Citation:

Bopp, L., M. Lévy, L. Resplandy, and J. B. Sallée (2015), Pathways of anthropogenic carbon subduction in the global ocean, *Geophys. Res. Lett.*, *42*, 6416–6423, doi:10.1002/2015GL065073.

Received 26 JUN 2015

Accepted 7 JUL 2015

Accepted article online 14 JUL 2015

Published online 6 AUG 2015

Pathways of anthropogenic carbon subduction in the global ocean

L. Bopp¹, M. Lévy², L. Resplandy^{1,3}, and J. B. Sallée²

¹LSCE-IPSL, CNRS/CEA/UVSQ, CEA Saclay, Gif-sur-Yvette, France, ²LOCEAN-IPSL, Sorbonne Université (UPMC, Paris 6)/CNRS/IRD/MNHN, France, ³Scripps Institution of Oceanography, University of California, San Diego, La Jolla, California, USA

Abstract The oceanic uptake of anthropogenic carbon is tightly coupled to carbon subduction, i.e., the physical carbon transfer from the well-ventilated surface ocean to its interior. Despite their importance, pathways of anthropogenic carbon subduction are poorly understood. Here we use an ocean carbon cycle model to quantify the mechanisms controlling this subduction. Over the last decade, 90% of the oceanic anthropogenic carbon is subducted at the base of the seasonally varying mixed layer. Vertical diffusion is the primary mechanism of this subduction (contributing 65% of total subduction), despite very low local fluxes. In contrast, advection drives the spatial patterns of subduction, with high positive and negative local fluxes. Our results suggest that vertical diffusion could have a leading role in anthropogenic carbon subduction, which highlights the need for an accurate estimate of vertical diffusion intensity in the upper ocean to further constrain estimates of the future evolution of carbon uptake.

1. Introduction

The ocean is a major sink of anthropogenic carbon thus slowing down the recent evolution of atmospheric CO₂ and climate change. Over the last decade (2004–2013), the ocean has absorbed 2.6 (±0.5) Pg C yr⁻¹, i.e., 27% of anthropogenic emissions from fossil fuel combustion (8.9 Pg C yr⁻¹) and land use changes (0.9 Pg C yr⁻¹) [Le Quéré *et al.*, 2014]. In the coming decades, the evolution of atmospheric CO₂ will strongly depend on how the ocean absorbs carbon.

The uptake of anthropogenic carbon is mainly a physical and chemical phenomenon, driven by increasing atmospheric CO₂ and by the resulting increasing partial pressure difference between the atmosphere and the surface ocean. The oceanic uptake of carbon is, however, limited by the amount of carbon in the upper layer of the ocean, and thus by the rate at which anthropogenic carbon, in the form of dissolved inorganic carbon (DIC), is subducted, i.e., transported from the well-ventilated surface ocean to the deep ocean [Sarmiento *et al.*, 1992; Graven *et al.*, 2012]. Carbon subduction is achieved by several physical mechanisms: vertical advection (including wind-driven Ekman pumping), horizontal advection across the sloping mixed-layer base, seasonal entrainment due to variations of the mixed-layer depth, and diffusion at the base of the mixed layer [Karleskind *et al.*, 2011].

Quantification of these mechanisms is not straightforward because it requires synoptic information on DIC distribution, ocean currents, mixed-layer depth, and diffusion rates. Using a combination of in situ and remote sensing observations and focusing on the Southern Ocean, Sallée *et al.* [2012] have shown that carbon subduction occurs in very specific locations (hot spots), which result from the interplay between the mean horizontal flow and sloping of the mixed-layer base (i.e., lateral induction). They also show that a significant fraction of the subducted anthropogenic carbon is reventilated back into the mixed layer, which needs to be taken into account to estimate the net sequestration.

Although the crucial role of subduction has been identified in key regions, an overview at the scale of the global ocean is still lacking. Because these processes largely depend on ocean circulation and on its changes in response to climate change and variability, the lack of knowledge of these processes casts doubt on the projections of the future evolution of ocean carbon uptake [Ciais *et al.*, 2014].

In this paper, we examine the anthropogenic carbon subduction at the scale of the global ocean. We adopt the approach of Lévy *et al.* [2013] who quantified the physical processes responsible for the transfers of carbon across the mixed-layer base using an ocean general circulation model. While Lévy *et al.* [2013] focused on

the transfer of natural carbon, we concentrate on anthropogenic carbon and decompose the total subduction into its components, i.e., advection, diffusion, and entrainment. The contribution of these different mechanisms is discussed at the global scale as well as regionally.

2. Method

The coupled hydrodynamical and biogeochemical model used in this study is NEMO (Nucleus for European Modelling of the Ocean) version 3.2 [Madec, 2008]. It couples the ocean dynamical code OPA [Madec, 2008], the sea-ice model LIM2 [Timmermann et al., 2005], and the marine biogeochemical model Pelagic Interaction Scheme for Carbon and Ecosystem Studies (PISCES) [Aumont and Bopp, 2006]. NEMO global configuration is used with a nominal horizontal resolution of 2° with increased 0.5° latitudinal resolution at the equator (ORCA2 grid). On the vertical, the grid has 31 levels with 10 levels in the upper 100 m. Mixing parameterizations include an explicit representation of mixed-layer dynamics, as well as a Laplacian viscosity, an isoneutral Laplacian diffusivity scheme, and the use of a Gent & McWilliams (GM) scheme to mimic the effect of subgrid-scale eddy processes [Gent and McWilliams, 1990]. Vertical diffusion coefficients K_z are derived from the Turbulent Kinetic Energy closure scheme of Blanke and Delecluse [1993], improved by Madec [2008] with additional parameterizations for Langmuir cells [Axell, 2002] and wind stirring [Rodgers et al., 2014]. The background K_z is set to $1.2 \cdot 10^{-5} \text{ m}^2 \text{ s}^{-1}$. Both the isoneutral diffusivity coefficient and the eddy-induced velocity coefficient are set to $2000 \text{ m}^2 \text{ s}^{-1}$.

PISCES (Pelagic Interaction Scheme for Carbon and Ecosystem Studies) [Aumont and Bopp, 2006] describes the cycle of carbon in the ocean and as such includes a simple representation of the marine ecosystem with four plankton types and phytoplankton limitations by five nutrients (Fe, Si, PO_4 , NO_3 , and NH_4). The carbonate chemistry follows the Ocean Carbon-Cycle Model Intercomparison Project protocols (www.ipsl.jussieu.fr/OCMIP) and CO_2 air-sea gas exchange is parameterized based on the Wanninkhof [1992] relationship for the gas transfer velocity.

NEMO-PISCES is initialized with the last year of the simulation described in Lévy et al. [2013], in which the model is forced by the CORE2 Normal Year Forcing [Large and Yeager, 2009] and by preindustrial atmospheric CO_2 . Here starting from this initial state, we first run a 60 year long spin-up simulation using the full 60 year CORE2 interannually varying forcing [Large and Yeager, 2009] and the same preindustrial atmospheric CO_2 . We then run an historical simulation, from 1888 to 2007, forced by atmospheric CO_2 concentration from 293 ppm to 382 ppm and forced by repeating two times CORE2 interannually varying forcing [Large and Yeager, 2009]. In addition to this historical simulation (referred to as ANTH), we also run a parallel simulation PIND forced by the same CORE2 physical forcing but in which atmospheric CO_2 is kept constant at its 1888 value.

To compute carbon subduction, we follow the approach proposed by Karleskind et al. [2011] that has been applied at the global scale to the transfer of natural carbon by Lévy et al. [2013]. In this approach, the subduction of carbon F_C is estimated at the base of the time-varying mixed layer by

$$F_C = \int_t \left[\underbrace{-(w_h + \mathbf{u}_h \cdot \nabla_H h) C_h}_{\text{vertical and lateral advection}} + \underbrace{(k_z \partial_z C)_h - C_h \cdot \partial_t h}_{\text{vertical mixing}} + \underbrace{F_{C \text{ eddies}}}_{\text{eddies}} \right] dt \quad (1)$$

where the first term on the right-hand side defines the total advection of carbon through the seasonally varying mixed-layer base with C_h , \mathbf{u}_h , and w_h as the values of dissolved inorganic carbon, horizontal velocity, and vertical velocity taken at the base of the mixed layer located at depth h . The second term in the right-hand side represents the contribution of vertical mixing, which is the sum of the vertical diffusion of carbon across the mixed-layer base with k_z being the vertical diffusion coefficient at the mixed-layer base, and of the vertical entrainment/detrainment of carbon due to local change in the mixed-layer depth h with time. This second term also includes the vertical component of the isopycnal diffusion. The third term corresponds to the role of eddies, which is parameterized following Gent and McWilliams [1990] with two terms: lateral diffusion along isoneutral surfaces and advection by a bolus velocity. Note that only the horizontal component of the isoneutral diffusion contributes to the eddy-induced flux $F_{C \text{ eddies}}$, as the vertical component is included in the vertical mixing term. Other terms that include fluxes of dissolved organic carbon or sinking of particles are omitted as they are similar with or without the addition of anthropogenic carbon in our model setup. In summary,

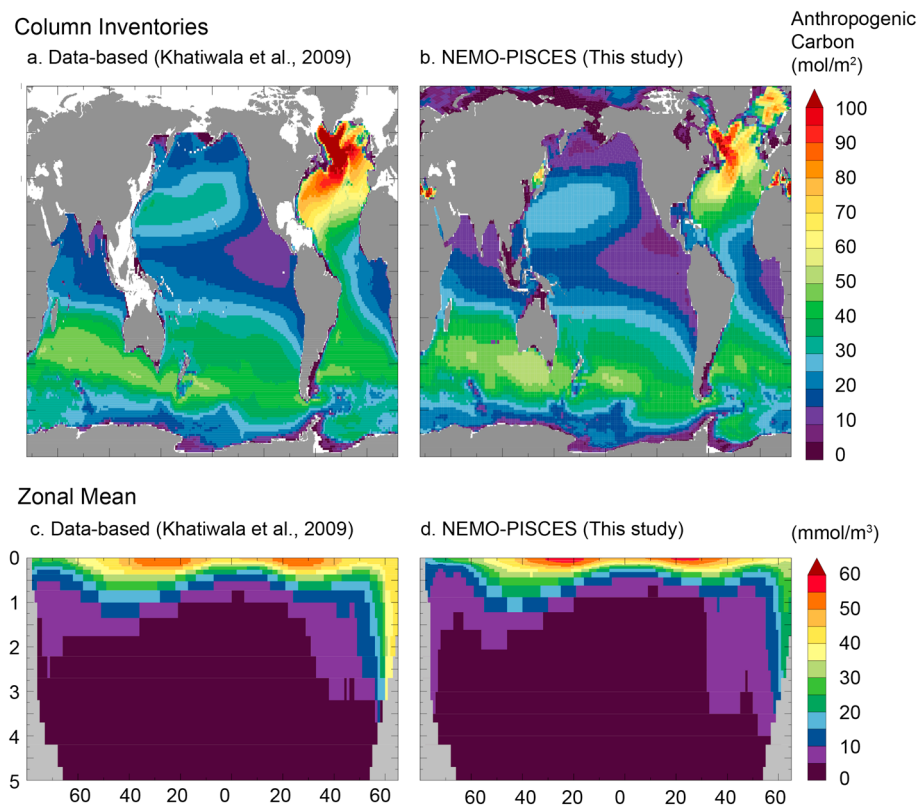


Figure 1. (a and b) Column inventories (mol m^{-2}) and (c and d) zonal mean (mmol m^{-3}) of anthropogenic carbon in 2007 estimated from the combination of observations and a green function method by *Khatiwala et al.* [2009] (Figures 1a and 1c) and as simulated with NEMO-PISCES (Figures 1b and 1d).

we decompose the annual C subduction across the time-varying mixed-layer into three types of physical processes: advection (lateral and vertical), vertical mixing (entrainment and vertical diffusion), and eddy transfer (lateral diffusion and bolus advection).

Anthropogenic carbon (C_{anth}) is defined as the excess amount of dissolved inorganic carbon present in seawater because of increasing atmospheric CO_2 compared to the preindustrial ocean. We thus take the difference between our two simulations ANTH and PIND to estimate C_{anth} .

3. Results

3.1. Air-Sea Flux and Ocean Storage of Anthropogenic Carbon

Over the last 18 years of our simulation period (1990–2007), the mean oceanic anthropogenic CO_2 sink, estimated from the difference between our two simulations ANTH and PIND, is $2.28 \text{ Pg C yr}^{-1}$. Our estimate of anthropogenic CO_2 sink compares well with the latest estimate of *Wanninkhof et al.* [2013], determined from a combination of observation-based approaches and ocean models and which amounts to 2.0 Pg C yr^{-1} for a similar period (1990–2009).

The total anthropogenic carbon inventory in the ocean, estimated for 2007 from the difference between our two simulations ANTH and PIND, amounts to 128.7 Pg C . When the carbon inventory of the model is integrated only over the regions covered by the observation-based carbon climatology Global Ocean Data Analysis Project (GLODAP) [*Key et al.*, 2004], which do not cover coastal regions and several marginal seas (including the Mediterranean Sea and the Arctic), the simulated total anthropogenic carbon inventory reduces to $114.7 \text{ Pg C yr}^{-1}$. This modeled anthropogenic carbon inventory is consistent with the observation-based estimate of *Khatiwala et al.* [2009, 2013], who estimated an anthropogenic carbon inventory of 121 Pg C yr^{-1} ($\pm 20\%$) over the same period (from 1888 to 2007) and the same regions (GLODAP regions).

The column inventories, as well as the global zonal mean, of anthropogenic carbon, simulated with NEMO-PISCES is comparable to the observation-based estimate of *Khatiwala et al.* [2009, 2013] (Figure 1).

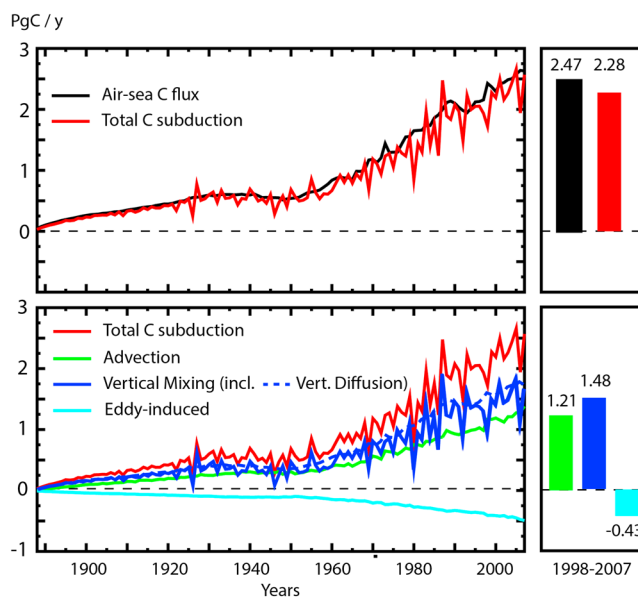


Figure 2. (top) Global integral of the anthropogenic carbon air-sea flux (black) and anthropogenic carbon subduction (red) in Pg C yr^{-1} . (bottom) The flux across the mixed-layer base interface is then decomposed into advection (green), vertical mixing (dark blue), and eddy-induced (light blue) components. The vertical diffusion component of vertical mixing is also shown (dark blue, dashed). On the right the decadal average over 1998–2007 of these different fluxes is shown. Fluxes are counted positively when directed from the atmosphere to the ocean, and from the surface to the deep ocean.

Both estimates show high inventories of C_{anth} in the North Atlantic (from 60 to 100 g C m^{-2}), even if slightly underestimated in our modeling approach as previously noticed for other modeling systems (e.g., Wang *et al.* [2012], for CCSM3.1). In the North Pacific, the accumulation of C_{anth} is lower, from 10 to 40 g C m^{-2} , and again slightly underestimated in the model. In the Southern Ocean, C_{anth} inventories reach 55 g C m^{-2} and are particularly well reproduced as compared to other models discussed in Khatiwala *et al.* [2013] and in which the physical ventilation of mode and intermediate waters has been shown to be too weak [Long *et al.*, 2013]. When spatially integrated, the Southern Ocean (south of 44°S) accounts for 20% of the global inventory (i.e., 24.5 Pg C in 2007), a similar proportion than in the Khatiwala *et al.* [2013] estimate.

3.2. Subduction of Anthropogenic Carbon

In 2007, the total amount of anthropogenic carbon stored below the annual-mean mixed-layer depth estimated from the difference between ANTH and PIND simulations, is 105 Pg C . It represents 90% of the total anthropogenic carbon in the ocean, which compares well with an observation-based estimate using Khatiwala *et al.* [2013] for anthropogenic carbon, and de Boyer Montegut *et al.* [2004] (updated) for the mixed-layer depth (91% for the proportion of anthropogenic carbon stored below the mixed layer).

The subduction of C_{anth} across the mixed-layer base has been estimated using the approach described in section 2. It amounts to $2.28 \text{ Pg C yr}^{-1}$ over the last simulated decade 1998–2007 (Figure 2), corresponding to 92% of the air-sea flux of anthropogenic carbon, thus very similar to the ratio of deep (below the annual-mean mixed-layer depth) over total anthropogenic carbon inventories. However, the flux of C_{anth} across the mixed-layer (ML) base displays much more time variability than the air-sea C_{anth} flux, with interannual standard deviation of $0.21 \text{ Pg C yr}^{-1}$ over 1990–2007 versus only $0.06 \text{ Pg C yr}^{-1}$ for that of air-sea C_{anth} flux. Note that when using the total air-sea CO_2 flux (including both the natural and anthropogenic components), the simulated interannual standard deviation then amounts to $0.24 \text{ Pg C yr}^{-1}$, in line with the most recent estimate of Wanninkhof *et al.* [2013], i.e., 0.2 Pg C yr^{-1} over 1990–2009.

We decompose the subduction of C_{anth} into its three major components (Figure 2). The dominant component responsible for the subduction of C_{anth} is vertical mixing, which encompasses both vertical entrainment/detrainment and vertical diffusion and amounts to $1.48 \text{ Pg C yr}^{-1}$, i.e., 65% of the total flux over 1998–2007. The advective component (comprising both horizontal and vertical terms) is $1.21 \text{ Pg C yr}^{-1}$. Finally, the eddy-induced component, estimated using the Gent and McWilliams parameterization, is negative

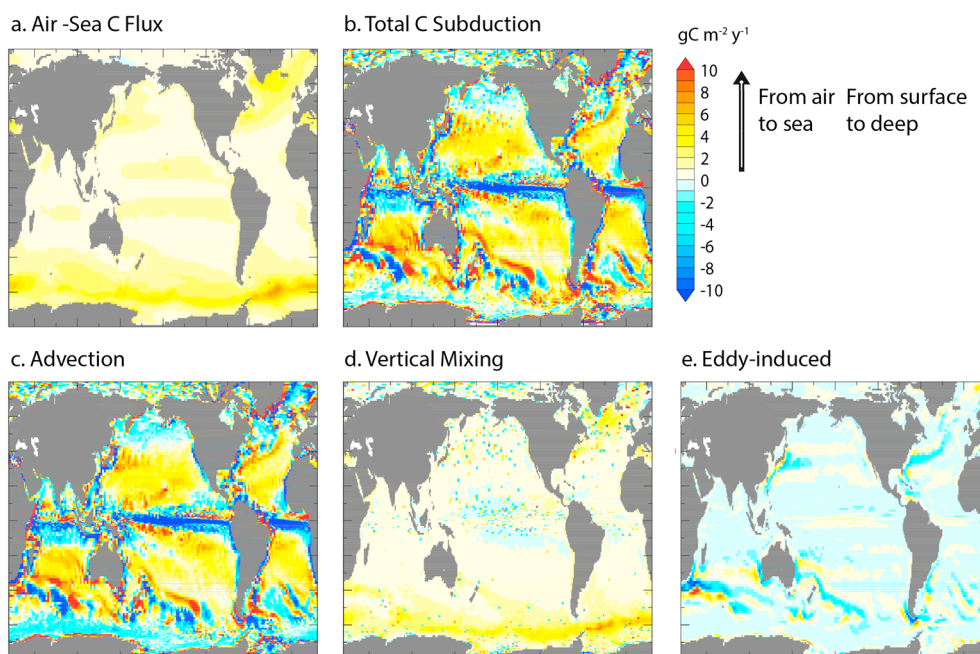


Figure 3. Spatial distribution of anthropogenic (a) carbon air-sea flux and (b) total anthropogenic carbon subduction. The subduction flux is then decomposed into (c) advection, (d) vertical mixing, and (e) eddy-induced components. Fluxes, in mol C m⁻² yr⁻¹, averaged over 1998–2007, are counted positively when directed from the atmosphere to the ocean, and from the surface to the deep ocean.

($-0.43 \text{ Pg C yr}^{-1}$), thus bringing back anthropogenic carbon from the subsurface to the surface layers of the ocean. Advection and vertical mixing components each represent between half and two thirds of the total transfer flux of C_{anth} . It is the vertical mixing component, driven by vertical entrainment/detrainment and hence variations of the mixed-layer depth, that is responsible for the large interannual variability of the total flux of C_{anth} across the ML base.

Although the amplitude of the air-sea flux and the subduction across the ML base are similar when integrated over the global ocean (Figure 2), their spatial distribution show striking differences (Figure 3). While air-sea C_{anth} fluxes are always positive, ranging from 0 to 3–4 g C m⁻² yr⁻¹ in the North Atlantic and the Southern Ocean, subduction rates display positive and negative fluxes, from -10 to 10 g C m⁻² yr⁻¹. This regional variability of the subduction flux illustrates the localized nature of the subduction of C_{anth} as well as the existence of large areas where C_{anth} is reventilated or obducted back into the mixed layer [Sallée *et al.*, 2012].

The spatial patterns of total subduction is largely dominated by the spatial variability of its advective component (Figure 3c). The two main large-scale characteristics of the advective fluxes are (1) a large reventilation region in the equatorial band surrounded on both sides by areas of subduction extending into the subtropical gyres and (2) regions of hot spots of subduction and reventilation mostly located in the Southern Ocean and in the North Atlantic. In the tropical band, advective fluxes across the ML base are controlled by the pathways of subtropical cells, which upwells subsurface waters and their C_{anth} into the ML in the equatorial band ($5^{\circ}\text{S}–5^{\circ}\text{N}$). In the Southern Ocean, the distribution of localized subduction/reventilation regions is controlled by the interplay between the gradients of mixed-layer depths and the mean lateral flow, as discussed in Sallée *et al.* [2012]. Finally, in the North Atlantic, subduction of C_{anth} is localized in the northern flank of the Gulf Stream, whereas obduction/reventilation occurs on its southern flank, demonstrating as well the interplay between mixed-layer depth gradients and lateral advection, as shown for nutrients by Williams *et al.* [2006]. These regional patterns are largely consistent with the known large-scale patterns of water masses subduction and obduction in the world's ocean [Lévy *et al.*, 2013].

The vertical mixing contribution to the total subduction of C_{anth} shares similar spatial patterns and flux intensities than air-sea C_{anth} fluxes (Figures 3a and 3d). Vertical mixing-induced subduction is always downwardly oriented and reaches values up to 3–4 g C m⁻² yr⁻¹ in the North Atlantic and the Southern Ocean. These fluxes

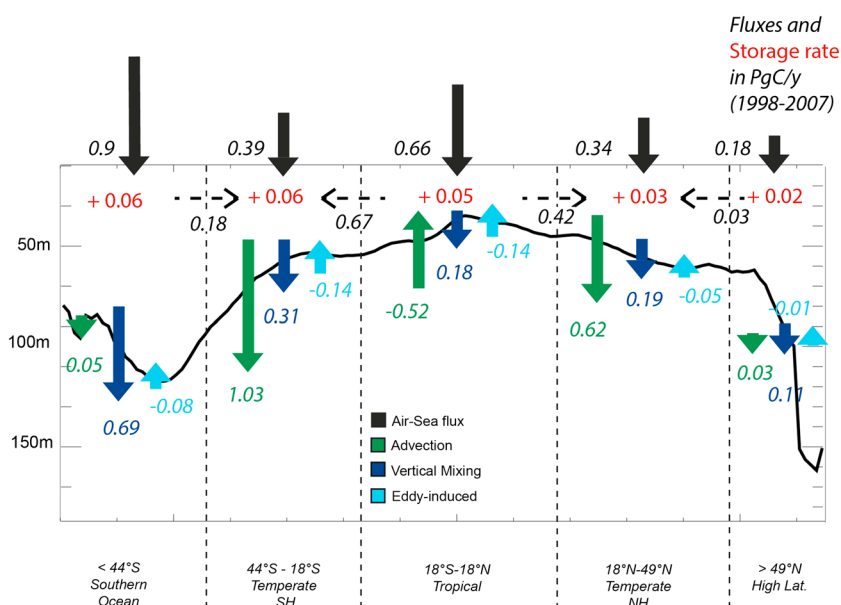


Figure 4. Regional integrals of anthropogenic carbon fluxes (in Pg C yr^{-1}), averaged over 1998–2007, across the air-sea interface (black) and across the mixed-layer base interface (total subduction) decomposed into advection (green), vertical mixing (dark blue), and eddy-induced (light blue) components. Storage rate of anthropogenic carbon in the mixed layer, also in Pg C yr^{-1} and for 1998–2007, is shown in red.

result mostly from vertical diffusion, vertical entrainment/detrainment contributing only to drive their high interannual variations (Figure 2). The magnitude of vertical diffusion at the base of the mixed layer ensues from vertical diffusion coefficients K_z of the order of $10^{-4} \text{ m}^2 \text{ s}^{-1}$ (resulting from a background K_z of $1.2 \cdot 10^{-5} \text{ m}^2 \text{ s}^{-1}$ augmented by the wind stirring parameterization just below the ML as described in Rodgers *et al.* [2014]), and vertical C_{anth} gradients of the order of 0.1 kg m^{-4} just below the ML base (corresponding to a vertical gradient of DIC of 10 kg m^{-3} per 100 m).

The eddy-induced contribution to C_{anth} subduction is highly localized and mostly negative (i.e., it leads to bring C_{anth} back into the mixed layer; see Figure 3e). The fact that this term is mostly negative is due to the preponderance of the bolus advection component in the eddy-induced term. It partly counteracts the advective component in the Gulf Stream, in the Kuroshio and also in the Antarctic Circumpolar Current region as previously shown by Sallée *et al.* [2012].

3.3. A Large-Scale Perspective on C_{anth} Subduction

When integrated over large zonal bands, the different pathways of C_{anth} subduction show contrasting terms (Figure 4):

1. The Southern Ocean contributes 40% of the net ocean uptake of C_{anth} , with 0.9 Pg C yr^{-1} over 1998–2007. Out of these 0.9 Pg C , 0.69 is subducted via vertical mixing, whereas 0.18 is transferred from the Southern Ocean into the southern temperate regions in the mixed layer.
2. The northern and southern temperate regions contribute moderately to the net ocean uptake of C_{anth} (0.34 and $0.39 \text{ Pg C yr}^{-1}$, respectively, over 1998–2007). They are, however, the main regions contributing to C_{anth} subduction, with 0.76 and $1.20 \text{ Pg C yr}^{-1}$ transferred across the ML base, respectively. These fluxes mostly occur via lateral/vertical advection, with vertical mixing only contributing one quarter of the total subduction.
3. Finally, the tropical region ($18^\circ\text{S} - 18^\circ\text{N}$), partly due its large extent, is a large contributor to the ocean uptake of C_{anth} , with a net air-to-sea carbon flux $0.66 \text{ Pg C yr}^{-1}$. It is, however, a region where a similar amount of anthropogenic carbon ($0.52 \text{ Pg C yr}^{-1}$) is advected back in the ML from below. Most of this anthropogenic carbon, from the atmosphere and from the ocean's interior, is transferred to the temperate regions within the mixed layer (0.42 and $0.67 \text{ Pg C yr}^{-1}$), to the temperate Northern and Southern Hemispheres, respectively.

4. Discussion and Conclusions

Anthropogenic carbon subduction is computed globally from a coupled hydrodynamical and carbon cycle model. Net air-sea fluxes of C_{anth} , as well as regional inventory of C_{anth} are in good agreements with observation-based estimates, providing us confidence that the model produces reasonable subduction rates. Total C_{anth} subduction is regionally much patchier than air-sea fluxes of C_{anth} . This is particularly true in the Southern Ocean, North Atlantic, and North Pacific basins, though the regional structures are much more pronounced in the Southern Ocean than anywhere else, in agreement with *Sallée et al.* [2012]. This regional patchiness is primarily due to the interplay between the sloping of the mixed-layer base and the mean flow, which ultimately produces successive regions of subduction and upwelling. Therefore, when a water parcel is subducted from the ocean surface to the interior, it can either be “permanently” (i.e., over long timescale) exported away from the surface or be reentrained in an upwelling region downstream of where it subducted. While beyond the scope of this study, a possible extension of the present work would be to isolate the region where subducted anthropogenic carbon is efficiently exported away from the surface for long timescale, which would involve following Lagrangian pathways of subducted waters [e.g., *Huang*, 1991; *ludicone et al.*, 2011].

Our study points out the potential role of eddies in the transfer of anthropogenic carbon to the intermediate and deep ocean. While eddy-induced transfer has been shown to be almost negligible for natural carbon [*Lévy et al.*, 2013], we find in this study that it is a significant term for the subduction of anthropogenic carbon, and it opposes the fluxes due to advection and vertical mixing. These results would need to be refined with the use of an eddy-resolving configuration instead of the coarse resolution model we use in this study. Consistent with our results, although they were focusing on meridional transport rather than subduction, *Ito et al.* [2010] showed from an eddy-permitting simulation that eddies partially compensate the mean northward flux of anthropogenic carbon due to Ekman transport.

The most novel aspect of our study probably concerns the role of vertical diffusion. Our model suggests vertical diffusion has a very significant role for the subduction of C_{anth} . We believe it might have been overlooked in previous studies because its local flux is usually much lower than other contributions (e.g., 2 orders of magnitude lower than that due to advection). However, since vertical diffusion of C_{anth} is consistently oriented downward, when summed up over large regions or globally, it results into a significant net flux. We note, however, two possible limitations about the interpretation of these vertical diffusion results. First, while subduction has often been discussed in terms of transfer across the base of the winter mixed layer (the water that escapes the seasonally ventilated layer) [e.g., *Stommel*, 1979; *Huang*, 1991; *Sallée et al.*, 2012], here we define the subduction as the water that crosses the instantaneous mixed layer, as in *Lévy et al.* [2013], where, by construction, gradients of tracers, such as C_{anth} , are larger. Our definition of subduction therefore naturally tends to give more weight to vertical diffusion as compared to other definitions of subduction. Second, the total subduction flux of C_{anth} is naturally adjusted by diffusive flux though the existence of a negative feedback between the diffusive flux of C_{anth} and the vertical gradient of C_{anth} at the base of the ML. Specifically, if the model misses important vertical transfer fluxes by advection, or eddy-induced processes, the concentration of C_{anth} will tend to climb in the surface layer, which would increase the vertical gradient of C_{anth} and therefore the vertical diffusion of C_{anth} . While this negative feedback effect makes diffusive flux dependent on the realism of the other subduction terms, we note that it also tends to reduce the dependency of our diffusion flux estimate to the exact choice of the K_z parameterization and parameter values, both extremely uncertain. As such, uncertainties on the value of K_z would not propagate entirely on the diffusive flux estimate due to the negative feedback involving the diffusive flux and the vertical gradient of C_{anth} .

Nonetheless, our study points out the possible importance of vertical diffusion and demonstrates the strong need of accurate estimates of vertical diffusion coefficients in the upper hundred meters of the ocean, as well as, a need to accurately estimate vertical gradients of C_{anth} over large spatial scale.

References

- Aumont, O., and L. Bopp (2006), Globalizing results from ocean in situ iron fertilization studies, *Global Biogeochem. Cycles*, 20, GB2017, doi:10.1029/2005GB002591.
- Axell, L. B. (2002), Wind-driven internal waves and Langmuir circulations in a numerical ocean model of the southern Baltic Sea, *J. Geophys. Res.*, 107(C11), 3204, doi:10.1029/2001JC000922.
- Blanke, B., and P. Delecluse (1993), Variability of the Tropical Atlantic ocean simulated by a general circulation model with two different mixed-layer physics, *J. Phys. Oceanogr.*, 23(7), 1363–1388.

Acknowledgments

We thank C. Ethé, O. Aumont, and P. Karleskind for their help, support, and comments on this manuscript. We thank S. Kathiwal for the use of data-based anthropogenic carbon estimates. The version of the NEMO code this study is based on is freely available at <http://www.nemo-ocean.eu/>. L.B. received support from the EU FP7 project CarboChange (contract 264879). J.B.S. received support from Agence Nationale de la Recherche (ANR), ANR-12-PDOC-0001.

The Editor thanks two anonymous reviewers for their assistance in evaluating this paper.

- Ciais, P., et al. (2014), Carbon and other biogeochemical cycles, in *Climate Change 2013: The Physical Science Basis. Contribution of Working Group I to the Fifth Assessment Report of the Intergovernmental Panel on Climate Change*, edited by T. F. Stocker et al., pp. 465–570, Cambridge Univ. Press, Cambridge, U. K., and New York.
- de Boyer Montégut, C., G. Madec, A. S. Fischer, A. Lazar, and D. Iudicone (2004), Mixed layer depth over the global ocean: An examination of profile data and a profile-based climatology, *J. Geophys. Res.*, *109*, C12003, doi:10.1029/2004JC002378.
- Gent, P., and J. McWilliams (1990), Isopycnal mixing in ocean circulation models, *J. Phys. Oceanogr.*, *20*, 150–155.
- Graven, H. D., N. Gruber, R. Key, S. Khatiwala, and X. Giraud (2012), Changing controls on oceanic radiocarbon: New insights on shallow-to-deep ocean exchange and anthropogenic CO₂ uptake, *J. Geophys. Res.*, *117*, C10005, doi:10.1029/2012JC008074.
- Huang, R. X. (1991), The three-dimensional structure of wind-driven gyres: Ventilation and subduction, *Rev. Geophys.*, *29*, 590–609.
- Ito, T., M. Woloszyn, and M. Mazloff (2010), Anthropogenic carbon dioxide transport in the southern ocean driven by Ekman flow, *Nature*, *463*(7277), 80–83, doi:10.1038/nature08687.
- Iudicone, D., K. B. Rodgers, I. Stendardo, O. Aumont, G. Madec, L. Bopp, O. Mangoni, and M. Ribera d'Alcala' (2011), Water masses as a unifying framework for understanding the Southern Ocean carbon cycle, *Biogeosciences*, *8*(5), 1031–1052, doi:10.5194/bg-8-1031-2011.
- Karleskind, P., M. Lévy, and L. Memery (2011), Subduction of carbon, nitrogen, and oxygen in the Northeast Atlantic, *J. Geophys. Res.*, *116*, C02025, doi:10.1029/2010JC006446.
- Key, R. M., A. Kozyr, C. L. Sabine, K. Lee, R. Wanninkhof, J. L. Bullister, R. A. Feely, F. J. Millero, C. Mordy, and T.-H. Peng (2004), A global ocean carbon climatology: Results from global data analysis project (GLODAP), *Global Biogeochem. Cycles*, *18*, GB4031, doi:10.1029/2004GB002247.
- Khatiwala, S., F. Primeau, and T. Hall (2009), Reconstruction of the history of anthropogenic CO₂ concentrations in the ocean, *Nature*, *462*(7271), 346–349, doi:10.1038/nature08526.
- Khatiwala, S., et al. (2013), Global ocean storage of anthropogenic carbon, *Biogeosciences*, *10*(4), 2169–2191, doi:10.5194/bg-10-2169-2013.
- Large, W. G., and S. G. Yeager (2009), The global climatology of an interannually varying air-sea flux data set, *Clim. Dyn.*, *33*(2–3), 341–364, doi:10.1007/s00382-008-0441-3.
- Le Quéré, C., et al. (2014), Global carbon budget 2014, *Earth Syst. Sci. Data Discuss.*, *7*(2), 521–610, doi:10.5194/essdd-7-521-2014.
- Lévy, M., L. Bopp, P. Karleskind, L. Resplandy, C. Ethé, and F. Pinsard (2013), Physical pathways for carbon transfers between the surface mixed layer and the ocean interior, *Global Biogeochem. Cycles*, *27*, 1001–1012, doi:10.1002/gbc.20092.
- Long, M. C., K. Lindsay, S. Peacock, J. K. Moore, and S. C. Doney (2013), Twentieth-century oceanic carbon uptake and storage in CESM1 (BGC), *J. Clim.*, *26*(18), 6775–6800.
- Madec, G. (2008), *NEMO Ocean Engine*, vol. 27, pp. 1–217, Note du Pole de modélisation de l'Institut Pierre-Simon Laplace, France.
- Rodgers, K. B., O. Aumont, S. E. Mikaloff Fletcher, Y. Plancherel, L. Bopp, C. de Boyer Montégut, D. Iudicone, R. F. Keeling, G. Madec, and R. Wanninkhof (2014), Strong sensitivity of Southern Ocean carbon uptake and nutrient cycling to wind stirring, *Biogeosciences*, *11*(15), 4077–4098, doi:10.5194/bg-11-4077-2014.
- Sallée, J.-B., R. J. Matear, S. R. Rintoul, and A. Lenton (2012), Localized subduction of anthropogenic carbon dioxide in the Southern Hemisphere oceans, *Nat. Geosci.*, *5*(8), 579–584, doi:10.1038/ngeo1523.
- Sarmiento, J. L., J. C. Orr, and U. Siegenthaler (1992), A perturbation simulation of CO₂ uptake in an ocean general circulation model, *J. Geophys. Res.*, *97*(C3), 3621–3645.
- Stommel, H. (1979), Determination of water mass properties of water pumped down from the Ekman layer to the geostrophic flow below, *Proc. Natl. Acad. Sci.*, *76*(7), 3051–3055.
- Timmermann, R., H. Goosse, G. Madec, T. Fichefet, C. Ethe, and V. Duliere (2005), On the representation of high latitude processes in the ORCA-LIM global coupled sea ice-ocean model, *Ocean Modell.*, *8*, 175–201.
- Wang, S., J. K. Moore, F. W. Primeau, and S. Khatiwala (2012), Simulation of anthropogenic CO₂ uptake in the CCSM3.1 ocean circulation-biogeochemical model: Comparison with data-based estimates, *Biogeosciences*, *9*(4), 1321–1336, doi:10.5194/bg-9-1321-2012.
- Wanninkhof, R. (1992), Relationship between wind speed and gas exchange over the ocean, *J. Geophys. Res.*, *97*, 7373–7382.
- Wanninkhof, R., et al. (2013), Global ocean carbon uptake: Magnitude, variability and trends, *Biogeosciences*, *10*(3), 1983–2000, doi:10.5194/bg-10-1983-2013.
- Williams, R. G., V. Roussenov, and M. J. Follows (2006), Nutrient streams and their induction into the mixed layer, *Global Biogeochem. Cycles*, *20*, GB1016, doi:10.1029/2005GB002586.